Toxicology Research

Accepted Manuscript

ROYAL SOCIETY OF CHEMISTRY

www.rsc.org/toxicology

Metabolomics reveals disturbed metabolic pathways in human lung epithelial cells exposed to airborne fine particulate matter

Qingyu Huang [a,b,*], Jie Zhang [a,b], Lianzhong Luo [c], Xiaofei Wang [a], Xiaoxue Wang [a], Ambreen Alamdar [a], Siyuan Peng [a], Liangpo Liu [a,b], Meiping Tian [a,b], Heqing Shen [a,b,*]

[a]*Key Laboratory of Urban Environment and Health, Institute of Urban Environment, Chinese Academy of Sciences, Xiamen 361021, PR China*

[b]*Ningbo Urban Environment Observation and Research Station-NUEORS, Chinese Academy of Sciences, Ningbo 315800, PR China*

[c]*Department of Pharmacy, Xiamen Medical College, Xiamen 361008, PR China*

***Corresponding author:** Institute of Urban Environment, Chinese Academy of Sciences, 1799 Jimei Road, Xiamen 361021, PR China.

Tel/Fax: (86)-592-6190771, E-mail: hqshen@iue.ac.cn (H. Shen)

Tel/Fax: (86)-592-6190523, E-mail: qyhuang@iue.ac.cn (Q. Huang)

Table of contents text:

Metabolomics was applied to unravel the metabolome alteration in A549 cells, and citrate cycle, amino acid biosynthesis and glutathione metabolism were the major metabolic pathways disturbed by airborne PM2.5.

ABSTRACT

Exposure to airborne fine particulate matter (PM2.5) has been associated with a variety of adverse health effects. However, the molecular mechanisms involved in PM2.5-elicited pulmonary toxicity are still not well elucidated. By conducting an ultra-high performance liquid chromatography/mass spectrometry based metabolomics analysis, the present study intended to investigate the alterations of metabolome in human lung epithelial cells (A549) exposed to PM2.5 extracts. In result, distinct metabolomic profiles were found to be associated with PM2.5 treatment. PM2.5 significantly changed the abundance of 16 intracellular metabolites in a dose-dependent manner, of which 13 were decreased and 3 were increased. By pathway analysis, it was shown that citrate cycle, amino acid biosynthesis and metabolism, and glutathione metabolism were the major metabolic pathways disturbed by PM2.5 in A549 cells. In addition, the expression changes of several key genes involved in these pathways further validated the metabolic alterations observed by metabolomics herein. It is suggested that PM2.5-induced oxidative stress may in part contribute to the perturbation of metabolic processes occurring in cell mitochondria. Overall, these results would be helpful to improve our understanding of the toxicological mechanisms related to PM2.5, and from such studies potential biomarkers indicative of inhalable PM2.5 exposure could be developed.

Introduction

Airborne particulate matter (PM)-caused air pollution has now raised great public concern due to its adverse health effects, which are greatly attributable to fine PM (PM2.5, aerodynamic diameter < 2.5 μm) exposure.[1] PM2.5 is mainly generated by gas-to-particle conversion mechanisms and condensation on to pre-existing particles in the accumulation-size mode. Numerous epidemiological studies have linked exposure to ambient PM2.5 with many health risks, including cardiovascular and pulmonary impairments,[2,3] diabetes,[4] reduced sperm quality,[5] adverse birth outcome,[6] as well as lung cancer.[7]

PM2.5 can deeply penetrate into respiratory tract and easily reach the alveolar ducts due to its small size. Therefore, lung is known as the primary target organ for PM2.5 exposure. Presently, the studies of PM2.5-induced lung toxicity have been widely performed on various cell lines and animal models. PM2.5 was shown frequently to induce oxidative stress by producing excessive intracellular reactive oxygen species (ROS), thereby causing DNA and mitochondrial damage,[8,9] chromosome alterations,[10] cell autophagy,[11] and abnormal release of inflammatory mediators closely involved in the development of lung diseases[12,13] Longhin et al.[14] found that PM2.5 induced severe cell cycle alterations, resulting in increased frequency of cells with double nuclei and micronuclei, followed by cell apoptosis. This effect is suggested to be related to the metabolic activation of PM2.5 organic chemicals, which cause damages to DNA and spindle apparatus. In addition, our recent proteomics study analyzed the global protein profile of A549 cells, and the expression of an array of proteins involved in oxidative stress, carbohydrate and energy metabolism, signal transduction, as well as protein synthesis and degradation were altered by PM2.5.[15]

Most of the findings mentioned above were mainly derived from conventional

single endpoint bioassays. 'Omics' technologies, which are capable to provide the information of global profile, are regarded as more powerful tools to investigate the toxicological responses to environmental exposure. There have been transcriptomics and proteomics studies of lung toxicity induced by PM2.5.[15,16] Because metabolic patterns-the end points of enzyme (protein) actions, are the final consequence of biological function, they may indicate aberrant physiological status more directly than genomic and proteomic profiles. Metabolomics can quantitatively measure the global metabolic response to environmental stimuli in living systems, and therefore enable toxicological mechanisms to be understood thoroughly.[17,18]

Several researches have addressed the effects of airborne PMs using metabolomics. Chen et al.[19] investigated the alterations of metabolic profile in lipids extracted from rat lung long-term exposed to ambient air, and decreased unsaturated PCs were observed, which may indicate the attack of ROS generated by PMs. Neal et al.[20] analyzed the hippocampus metabolome of mouse pups with cigarette smoke exposure during development, and found that the altered metabolites were mainly involved in glycolysis, oxidative phosphorylation and fatty acid metabolism. Another study was performed to decipher the effects of welding fumes on the plasma metabolome in exposed workers. The results revealed an association of high-dose exposure to metal fumes with reduced unsaturated fatty acids.[21] It is known that different PMs have different toxicity, due to their distinctions in particle size and toxic components.[2] To date, however, metabolic signatures are still rarely characterized for PM2.5 exposure.

For this purpose, the present study was designed to investigate the metabolomic alterations in human lung epithelial cells (A549), a widely applied *in vitro* model for the studies of PM2.5-induced lung toxicity,[9,11,15] following PM2.5 exposure using a metabolomics approach based on ultra-high performance liquid chromatography/mass

spectrometry (UPLC/MS). Furthermore, the expression levels of key genes involved in the altered metabolic pathways were also examined. These results may be worthy to yield novel insights into the mechanisms regarding PM2.5-mediated pulmonary toxicity, and to screen biomarker candidates indicating ambient PM2.5 exposure.

Materials and methods

Collection, extraction and chemical characterization of PM2.5

Airborne PM2.5 was collected using a HiVol 3000 air sampler (Ecotech, Australia) on the rooftop of Institute of Urban Environment, Chinese Academy of Sciences, which is located in a suburban region with rapid urbanization, surrounded by highways, schools, residential buildings in construction and a sea bay in Xiamen City, China. The sampler was set on the rooftop of a building, about 30 m above the ground, and the sampling was performed every 24 h from 20 to 23 October in 2011. The pooled PM2.5 samples during the whole sampling periods were retained on the fiber filters. The filters were weighted and the density of PM2.5 on the filter was calculated as 1 mg/cm^2. For extraction, a portion of filter (20 cm^2, 20 mg PM2.5) was cut into small pieces and immersed in ultrapure water. After ultrasonic extraction (30 min each time, 6 times), the filters were removed and the resulting liquid was dried and stored at -80°C for further use. The chemical characteristics (elements, inorganic ions and polycyclic aromatic hydrocarbons) of PM2.5 extracts have been described in our previous report.[15]

Cell culture and PM2.5 exposure

Human lung epithelial cells, A549 (ATCC® CCL-185) were routinely maintained in RPMI 1640 medium (Gibco, USA), supplemented with 10% inactivated fetal bovine serum (Gibco, USA) and 1% penicillin/streptomycin (Gibco, USA) and cultured in an incubator at 37°C, supplied with 5% CO_2. For exposure, the dried PM2.5 extracts

were weighted and dissolved in sterilized water to obtain the liquid extracts at a final concentration of 4000 mg/L. The 72 h-IC50 of PM2.5 to A549 cells was calculated as 120 mg/L by our previous MTT assay.[15] Therefore, A549 cells at exponential phase (about 10^6 cells) were then treated with 30 and 60 mg/L of PM2.5 for 72 h, at which cell viability was 81.5% and 69.1%, respectively. The cells treated with sterilized water were served as control. The control and each exposure group were six replicates.

Sample preparation

After exposure, the medium was removed and the cells were washed twice with PBS. Then, 1 mL of 80% (v/v) methanol solution stored in -80 ◦C was added to quench the enzymatic reactions in cells. After being incubated at -80 ◦C for 15 min, the cells were scraped and collected in a centrifuge tube. Cell lysates were prepared with ultrasonication (200 W, sonication for 5 s, interval for 10 s, 50 cycles) and centrifugation at 12,000 rpm, 4 ◦C for 10 min. The supernatants were dried using a Speedvac concentrator (Thermo Fisher Scientific, NC, USA), and then reconstituted with 100 μL of 10% (v/v) methanol. The samples were centrifuged at 12,000 rpm, 4 ◦C for 15 min, and the supernatants were collected for LC/MS analysis.[22] A quality control (QC) sample was prepared by mixing aliquots of each sample and therefore broadly representative of the whole sample set.

LC/MS analysis

Metabolic profiling was conducted using a Waters ACQUITY UPLC system (Waters, Milford, MA, USA) coupled to a Q Exactive mass spectrometer (Thermo Fisher, USA). Chromatographic separation was performed on an ACQUITY UPLC BEH C18 column (1.7 μm, 100 mm × 2.1 mm i.d.) (Waters, Milford, MA, USA). For each sample, the run time was 20 min at a flow rate of 0.4 mL/min. The mobile phases

were (A) methanol with 0.1% formic acid and (B) H_2O with 0.1% formic acid. The programmed gradient was 0 min, 0% A; 6 min, 25% A; 10 min, 80% A; 12 min, 100% A; 15 min, 100% A; 15.5 min, 0% A; and 20 min, 0% A. The column was maintained at 50 °C and the injection volume was 5 μL.

The mass spectrometer equipped with heated electrospray ionization (HESI) source was operated in positive or negative ion mode with a scan range of 100 to 1000 *m/z*. Spray voltage was set at 3500 V for positive mode and 2500 V for negative mode. Probe heater temperature was set at 425 °C, and capillary temperature was set at 262.5 °C. Nitrogen gas was used as carrier gas. The flow rate of sheath gas, aux gas and sweep gas was 50, 12.5 and 1 L/min, respectively. Data was collected in centroid mode. All the samples were run in a randomized fashion to remove possible uncertainties from artifact-related injection order and gradual changes of instrument sensitivity in batch runs. One QC sample was injected at the start the analytical batch, followed by analysis at every 6 sample injection throughout the running sequence. MS/MS mode was used to identify potential biomarkers with argon as collision gas. MS/MS was performed by normalized collision energy (NCE) technology with 30% NCE for the biomarkers with 17500 resolution and isolation window *m/z* of 1.0.

Data analysis

UPLC-MS data were processed with SIEVE software (Thermo Fisher Scientific, NC, USA) to generate a two-dimensional data table of ion peaks (*m/z*-retention time pairs) and their respective intensities (peak areas). Peak detection, retention time correction and alignment were performed using the following parameters: mass range of 100-1000 m/z, mass tolerance of 20 ppm, retention time (RT) range of 0.4-18.5 min, and RT width threshold of 0.2 min. All data in the table was normalized to total intensities to eliminate systematic bias, and any variables with missing values in more

than 20% of the samples were excluded. Finally, the processed tables were Pareto-scaled and submitted to SIMCA-P V11.5 software (Umetrics, Uppsala, Sweden) for multivariate statistical analysis. Principal component analysis (PCA) was first performed to discover intrinsic treatment-related clusters within the datasets. Following this, partial least-squares discriminant analysis (PLS-DA) was used to improve separation among the groups and screen biomarkers. A cross validation procedure and testing with 999 permutations were performed to avoid the over-fitting of supervised PLS-DA model. Variable importance in projection (VIP) represents the extracted variables' ability to discriminate different doses, and the variables with VIP values greater than 1.0 were included in the preset of biomarkers.[23] Metabolite identification based on UPLC-MS data was carried out according to Zhang et al.[24] Briefly, a sample was subjected to MS and MS/MS analysis to acquire accurate mass, isotopic pattern, and fragment ions for target metabolites. The structure information was then obtained by searching Human Metabolome Database (HMDB, http://www.hmdb.ca) based on accurate mass measurement with negative ion mode. An accepted mass difference of 20 mDa was set during the search. Furthermore, the UPLC/MS/MS product ion spectrum of metabolites was matched with the MS spectra available in HMDB to confirm the identification (Table S1, Supplementary data).

Quantitative real-time PCR

Total RNAs were extracted using the RNeasy® Mini Kit (Qiagen) from A549 cells. Reverse transcription of cDNA synthesis was performed with 1 μg of RNA using PrimeScript® RT reagent Kit with gDNA Eraser cDNA synthesis Kits (Takara, Japan). Real-time PCR was carried out in a 20 μL reaction mixture and performed in triplicate using SYBR Green Master Mix reagents (Roche, USA) on a Roche LightCycler® 480 Ⅱ real-time PCR system (Roche, USA) following the manufacturer's protocol (95 ◦C

for 10 min followed by 40 cycles at 95 ◦C for 15 s, and 60 ◦C for 30 s). Gene expression levels were normalized to GAPDH gene level. All primer sets are described in Table 1. Three replicates for each group were performed. The fold changes (treated/control) of the tested genes were analyzed by the $2^{-\Delta\Delta CT}$ method.

Statistical analysis

The data are all expressed as mean ± standard deviation (SD), and the statistical analysis was performed with SPSS software (Version 18.0). Significant differences among multiple groups were determined using a one-way analysis of variance (ANOVA) followed by LSD *post-hoc* test. Probabilities of $p < 0.05$ were considered as statistically significant.

Results

Metabolomic profiling

The metabolic profiles of A549 cells were acquired under positive or negative ion mode using UPLC/MS (Fig. 1). A total of 721 and 515 metabolic features were obtained under positive and negative ion mode, respectively. In order to assess the stability and reproducibility of the analytical instrument and sample carryover, a QC sample was injected at the beginning of the sequence and injected at regular intervals (every 6 samples) during the workflow. In addition, the coefficient of variation (CV) values of peak areas was less than 30% in 91.4% of the variables for positive ion mode, and in 86.4% of those for negative mode across the QC samples (Fig. S1, Supplementary data). All the results indicated that the method was robust with good dataset quality for further analysis.[25]

Multivariate statistical analysis of metabolic profiles

PCA was initially performed on the LC-MS datasets to visualize general clustering trends among the observations. Although there did not appear to be a clear segregation

of the metabolomic profiles of PM2.5-treated group from the controls, a tendency of intergroup separation was found in the scores plot for negative mode (Fig. 2A) but not for positive one (Fig. S2, Supplementary data). A supervised PLS-DA model was further used to discover the difference among different groups for negative mode (Fig. 2B). However, the model can't be successfully established for positive mode, indicating little difference among these metabolites. Therefore, the subsequent results were only described for negative mode.

As can be seen in Fig. 2B, the PM2.5-exposed groups (30 and 60 mg/L) were clearly discriminated from control group by the first two components based on models with $R^2Y = 0.771$ and $Q^2(cum) = 0.58$, indicating a faithful representation of the data and a good predictive ability of the model. In addition, the PLS-DA model was validated by a permutation test (999 random permutations), and no overfitting of the data was observed (Fig. S3, Supplementary data). These results suggested that PM2.5 exposure led to significant metabolic alterations in A549 cells.

Biomarker screening and identification

Extracted variables that contributed the most in group distinction were chosen as the biomarkers of PM2.5 exposure. Strict criteria were adopted in the screening: (1) 113 variables with a VIP value > 1 were brought into the superset of biomarkers; (2) then the number of candidates was reduced to 110 to meet the jack-knifing confidence interval > 0 (Fig. S4, Supplementary data); and (3) the difference of candidate levels (relative peak area) was statistically significant ($p<0.05$) between the control and treatment groups, and the fold change was dose-dependent. Following the criterion above, 23 variables were incorporated into the biomarker subset and 16 altered metabolites were identified and listed in Table 2. Among these, 13 metabolites were decreased while 3 were increased by PM2.5 treatment.

Metabolic pathways disturbed by PM2.5 in A549 cells

To obtain an overview of the effects of PM2.5 exposure on A549 cells, the metabolic pathways involved in the differential metabolites were analyzed using the web-based MetaboAnalyst 2.0 software (http://www.metaboanalyst.ca). The HMDB ID of 16 metabolites (Table 2) was imported to the pathway analysis module. As a result, the software generated 6 metabolic pathways with a p-value < 0.05 (Table S2, Supplementary data), which were considered to be significantly associated with PM2.5-induced metabolic changes.[20] These 6 pathways were characterized as nitrogen metabolism, citrate cycle, aminoacyl-tRNA biosynthesis, phenylalanine, tyrosine and tryptophan biosynthesis, glutathione metabolism, glyoxylate and dicarboxylate metabolism (Fig. 3). In brief, citrate cycle, amino acid biosynthesis, and glutathione metabolism were the 3 major metabolic pathways disturbed by PM2.5 in A549 cells.

Gene expression of key enzymes involved in the altered metabolic pathways

To validate the metabolic alterations, the expressions of key enzymes involved in these metabolic pathways were determined at gene level using quantitative real-time PCR analysis, including aconitase 2 (ACO2), isocitrate dehydrogenase [NADP] (IDH2), fumarase (FH), ATP synthase (ATP5C1), glutamate dehydrogenase (GLUD1), glutathione peroxidase (GPX1) and superoxide dismutase [Mn] (SOD2). As shown in Fig. 4, in citrate cycle, the upregulation of ACO2, FH and ATP5C1 was observed, whereas the level of IDH2 showed a decreased trend. GLUD1, which is related to glutamic acid biosynthesis, was significantly reduced by 1.5-fold. Moreover, GPX1 and SOD2, the genes indicated oxidative stress in mitochondrion, were both elevated in cells following PM2.5 exposure (Fig. 5).

Discussion

Although oxidative stress has been identified as one of the major risk factors, the

molecular mechanisms of PM2.5-induced pulmonary toxicity remain largely unclear. Toxicometabolomics seeks to identify critical metabolites and pathways in biological systems that are affected by and respond to adverse chemical or environmental stress using global metabolic profiling technologies.[26,27] It therefore, is able to augment our understanding of the toxic mechanisms involved in PM2.5 exposure besides genomic and proteomic studies. Furthermore, our recent study has pointed out that lung cell metabolism was disturbed by PM2.5.[15] However, the reports of metabolomic analysis using PM2.5 as a single toxin are seldom mentioned. In view of this, our study applied metabolomics approaches to reveal the metabolic alterations of A549 cells in response to PM2.5 exposure. A total of 16 potential biomarkers with statistically significant changes were identified. Moreover, the significantly perturbed metabolic pathways associated with PM2.5 treatment were characterized as citrate cycle, amino acid biosynthesis and metabolism, as well as glutathione metabolism (Fig. 6). The effects of PM2.5 exposure on these pathways were mainly discussed as follows.

The citrate cycle is central to aerobic metabolism, facilitating adequate throughout of substrates derived from carbohydrates, fatty acids or amino acids. Changes in two pivotal intermediates of citrate cycle were observed in this study. The levels of *cis*-aconitate and malate both decreased, which indicated the lowered citrate cycle level in PM2.5-treated A549 cells. It is known that the generation of *cis*-aconitate and malate depends on aconitase (ACO) and fumarase (FH). However, real-time PCR analysis showed that ACO2 and FH both were upregulated, suggesting that the depletion of *cis*-aconitate and malate may be caused by other factors. Pantothenate, a precursor of acetyl-CoA in mammalian cells,[28] was also reduced by PM2.5, indicating that metabolic processes utilizing acetyl-CoA may have been altered. Since citrate is produced from oxaloacetate and acetyl-CoA, it is presumed that the decrease of

pantothenate would impair the generation of citrate. In addition, ADP activates the activity of isocitrate dehydrogenase (IDH) while ATP is an inhibitor of this enzyme. Here, ADP was found to decrease in cells with PM2.5 exposure. Together with the upregulation of ATP5C1, we proposed that ATP has been elevated, which may lead to the inhibition of IDH2 followed by depletion of α-ketoglutarate. In support of our results, Vulimiri et al.[29] demonstrated that cigarette smoke exposure altered the abundance of citrate, α-ketoglutarate and malate in A549 cells.

The current study showed that PM2.5 changed the abundance of several amino acids including glutamate, *N*-Acetylglutamic acid (NAcGlu), phenylalanine and tryptophan in A549 cells. Lowered levels of citrate cycle biochemicals are consistent with reduced availability of amino acids for transamination entry into the cycle. As is expected, glutamate was reduced in response to PM2.5 exposure, which may be ascribed to the downregulation of α-ketoglutarate and glutamate dehydrogenase (GLUD1). Glutamate is known as the precursor for glutamine, proline and arginine, indicating that the biosynthesis of these amino acids would be weakened due to glutamate reduction. NAcGlu, which activates carbamoyl phosphate synthetase in the urea cycle, is biosynthesized from glutamate and acetyl-CoA. Not surprisingly, intracellular NAcGlu concentration decreased owing to the decreases of glutamate and acetyl-CoA, and deficient NAcGlu may subsequently impact on urea cycle.

Phenylalanine and tryptophan are two essential amino acids that cannot be synthesized by humans, and both of them showed a significant increase in A549 cells under PM2.5 stress. Knowing that phenylalanine is a precursor for tyrosine, we predict that the biosynthesis of tyrosine would be interfered. Consistent with our results, various amino acids including glutamate were reported to be changed by inhalable PMs *in vivo* and *in vitro*.[29,30] Furthermore, the expression levels of many

genes involved in phenylalanine and tyrosine were modulated in human bronchial epithelial cells exposed to PM2.5.[31] Amino acids are not only the composition of proteins, but also materials for energy metabolism and precursors of many metabolic intermediates.[32] Glutamate can be reversely metabolized into α-ketoglutarate; phenylalanine can be transformed into fumarate and acetyl-CoA; and tryptophan transformed into acetyl-CoA. Thus, the alterations of these amino acids will perturb protein biosynthesis and affect related metabolic pathways, such as citrate cycle in lung cell.

Oxidative stress has been considered fundamental in the biological effects seen after exposure to PM2.5. Glutathione (GSH) is an efficient antioxidant providing protection against oxidative stress through conjugation of electrophiles and reduction of ROS. Reduced GSH is transformed into oxidized GSH (GSSG) by the catalysis of glutathione peroxidase (GPX), and oxidative stress occurred in cells often causes rapid depletion of GSH with efflux of GSSG.[33] Many reports have revealed that oxidative damage induced by airborne particles including PM2.5 was characterized by reduction of GSH/GSSG ratio and regulated expression of various antioxidant enzymes.[34-36] Organic extracts from PM2.5 also affected the expressions of genes involved in GSH metabolism in human embryonic lung fibroblasts.[16] Consistently, this study observed the elevation of GSSG, which may be attributable to GPX1 upregulation, implying the oxidative damage to A549 cells with PM2.5 exposure. The result is also supported by our previous observation that PM2.5 induced excessive ROS generation in A549 cells.[15] In addition, mitochondria are both a sensitive target and a primary source of oxidative stress. PMs were reported to cause oxidative stress followed by mitochondrial damage and malfunctioning.[37,38] Our findings further showed that the expression of superoxide dismutase [Mn] (SOD2), a specific

antioxidant enzyme in mitochondria, was remarkably enhanced by PM2.5. Taken together, these results confirmed that PM2.5 induced oxidative damage in mitochondria, which probably led to the disturbance of citrate cycle and amino acid biosynthesis and metabolism in A549 cells.

It is well known that PM2.5 sampled from different localities or at different time will cause different degrees of toxicity due to their variations in chemical constitutes.[3] Considering the characters of the sampling site, it is proposed that the current sample may be representative of PM2.5 pollution of suburban regions with rapid urbanization in a coastal city in Southeastern China, and the toxicological data obtained herein could reflect the lung toxicity of such a specific PM2.5 sample. Since PM2.5 extracts are real complex mixtures, it is difficult to determine what roles each component plays in the cytotoxicity. However, in view of the dominant contents of metal constituents in the current extracts,[15] it is tempting to suggest that metallic coactions may contribute greatly to PM2.5-induced metabolic toxicity.

In summary, using a LC-MS based metabolomics analysis, the present study aimed to unravel the alterations of metabolic profiles in A549 cells exposed to PM2.5. As a result, 16 metabolites with dose-dependent changes in their intracellular abundance were identified and considered as potential biomarkers. Concerning their biological functions, the metabolic pathways mainly disrupted by PM2.5 were involved in citrate cycle (*cis*-aconitate, malate, pantothenate and ADP), amino acid biosynthesis and metabolism (glutamate, NAcGlu, phenylalanine and tryptophan), and oxidative stress (GSSG). We suggest that PM2.5 induced mitochondrial oxidative damage in A549 cells, which may result in perturbation of other metabolic processes (Fig. 6). The data obtained here would be useful supplements to our knowledge of the mechanisms underlying pulmonary toxicity mediated by airborne PM2.5 exposure.

Acknowledgments

This work was financially supported by the Knowledge Innovation Program of the Chinese Academy of Sciences (IUEQN201301, IUEZD201401), the Ningbo Science and Technology Fund (2013A610189, 2014A610284), and the National Nature Science Foundation of China (21307127).

Supplementary data

MS/MS information of identified differential metabolites (Table S1). Metabolic pathways significantly altered by PM2.5 in A549 cells (Table S2). Coefficients of variation (CVs) of the variables extracted from metabolic profiles of A549 cells (Fig. S1). Scoring plots of intracellular metabolites from A549 cells with PCA model under positive ion mode (Fig. S2). Random permutation test results (n = 999) of the PLS-DA model (Fig. S3). Variable influence in projection (VIP) plots of established PLS-DA model (Fig. S4).

References

1 C. A. 3rd Pope, D. W. Dockery, *J. Air Waste Manag. Assoc.*, 2006, **56,** 709-742.

2 S. Wu, F. Deng, H. Wei, J. Huang, H. Wang, M. Shima, X. Wang, Y. Qin, C. Zheng, Y. Hao, X. Guo, *Part. Fibre Toxicol.*, 2012, **9,** 49.

3 S. Wu, F. Deng, H. Wei, J. Huang, X. Wang, Y. Hao, C. Zheng, Y. Qin, H. Lv, M. Shima, X. Guo, *Environ. Sci. Technol.*, 2014, **48,** 3438-3448.

4 S. K. Park, W. Wang, *Curr. Environ. Health Rep.*, 2014, **1,** 275-286.

5 A. Hammoud, D. T. Carrell, M. Gibson, M. Sanderson, K. Parker-Jones, C. M. Peterson, *Fertil. Steril.*, 2010, **93,** 1875–1879.

6 S. Ha, H. Hu, D. Roussos-Ross, K. Haidong, J. Roth, X. Xu, *Environ. Res.*, 2014, **134C,** 198-204.

7 G. B. Hamra, N. Guha, A. Cohen, F. Laden, O. Raaschou-Nielsen, J. M. Samet, P. Vineis, F. Forastiere, P. Saldiva, T. Yorifuji, D. Loomis, *Environ. Health Perspect.*, 2014, **122,** 906-911.

8 N. Li, C. Sioutas, A. Cho, D. Schmitz, C. Misra, J. Sempf, M. Wang, T. Oberley, J. Froines, A.

Nel, *Environ. Health Perspect.*, 2003, **111,** 455–460.

9 E. Corsini, S. Budello, L. Marabini, V. Galbiati, A. Piazzalunga, P. Barbieri, S. Cozzutto, M. Marinovich, D. Pitea, C. L. Galli, *Arch. Toxicol.*, 2013, **87,** 2187-2199.

10 F. Saint-Georges, G. Garçon, F. Escande, I. Abbas, A. Verdin, P. Gosset, P. Mulliez, P. Shirali, *Toxicol. Lett.*, 2009, **187,** 172–179.

11 X. Deng, F. Zhang, W. Rui, F. Long, L. Wang, Z. Feng, D. Chen, W. Ding, *Toxicol. in Vitro*, 2013, **27,** 1762-1770.

12 Z., Dagher, G. Garçon, P. Gosset, F. Ledoux, G. Surpateanu, D. Courcot, A. Aboukais, E. Puskaric, P. Shirali, *J. Appl. Toxicol.*, 2005, **25,** 166–175.

13 P. A. Potnis, R. Mitkus, A. Elnabawi, K. Squibb, J. L. Powell, *Toxicol. Res.*, 2013, **2,** 259–269.

14 E. Longhin, J. A. Holme, K. B. Gutzkow, V. M. Arlt, J. E. Kucab, M. Camatini, M. Gualtieri, *Part. Fibre Toxicol.*, 2013, **10,** 63.

15 Q. Huang, J. Zhang, S. Peng, M. Tian, J. Chen, H. Shen, *J. Appl. Toxicol.*, 2014, **34,** 675-687.

16 H. Líbalová, K. Uhlířová, J. Kléma, M. Machala, R. J. Šrám, M. Ciganek, J. Topinka, *Part. Fibre Toxicol.*, 2012, **9,** 1.

17 M. Bouhifd, T. Hartung, H. T. Hogberg, A. Kleensang, L. Zhao, *J. Appl. Toxicol.*, 2013, **33,** 1365-1383.

18 N. J. Plant, *Toxicol. Res.*, 2015, **4,** 9–22.

19 W. L. Chen, C. Y. Lin, Y. H. Yan, K. T. Cheng, T. J. Cheng, *Mol. Biosyst.*, 2014. **10,** 3163-3169.

20 R. E. Neal, J. Chen, R. Jagadapillai, H. Jang, B. Abomoelak, G. Brock, R. M. Greene, M. M. Pisano, *Toxicology*, 2014, **317,** 40-49.

21 Y. Wei, Z. Wang, C. Y. Chang, T. Fan, L. Su, F. Chen, D. C. Christiani, *PLoS One*, 2013, **8,** e77413.

22 S. Peng, L. Yan, J. Zhang, Z. Wang, M. Tian, H. Shen, *J. Pharm. Biomed. Anal.*, 2013, **86,** 56-64.

23 C. Wang, R. Feng, Y. Li, Y. Zhang, Z. Kang, W. Zhang, D. J. Sun, *Toxicol. Lett.*, 2014, **229,** 474-481.

24 J. Zhang, X. Mu, Y. Xia, F. L. Martin, W. Hang, L. Liu, M. Tian, Q. Huang, H. Shen, *J. Proteome Res.*, 2014, **13,** 3088-3099.

25 E. J. Want, I. D. Wilson, H. Gika, G. Theodoridis, R. S. Plumb, J. Shockcor, E. Holmes, J. K. Nicholson, *Nat. Protoc.*, 2010, **5,** 1005-1018.

26 H. Shen, W. Xu, J. Zhang, M. Chen, F. L. Martin, Y. Xia, L. Liu, S. Dong, Y. G. Zhu, *Environ. Sci. Technol.*, 2013, **47,** 8843-8851.

27 J. Zhang, H. Shen, W. Xu, Y. Xia, D. B. Barr, X. Mu, X. Wang, L. Liu, Q. Huang, M. Tian, *Environ. Sci. Technol.*, 2014, **48,** 12265−12274.

28 R. Leonardi, Y. M. Zhang, C. O. Rock, S. Jackowski, *Prog Lipid Res.*, 2005, **44,** 125–153.

29 S. V. Vulimiri, M. Misra, J. T. Hamm, M. Mitchell, A. Berger, *Chem. Res. Toxicol.*, 2009, **22,** 492-503.

30 J. Z. Hu, D. N. Rommereim, K. R. Minard, A. Woodstock, B. J. Harrer, R. A. Wind, R. P. Phipps, P. *J. Sime, Toxicol. Mech. Methods*, 2008, **18,** 385-398.

31 X. Ding, M. Wang, H. Chu, M. Chu, T. Na, Y. Wen, D. Wu, B. Han, Z. Bai, W. Chen, J. Yuan, T. Wu, Z. Hu, Z. Zhang, H. Shen, *Toxicol. Lett.*, 2014, **228,** 25-33.

32 W. Liao, G. Tan, Z. Zhu, Q. Chen, Z. Lou, X. Dong, W. Zhang, W. Pan, Y. Chai, *J. Proteome Res.*, 2012, **11,** 5109-5123.

33 I. Rahman, X. Y. Li, K. Donaldson, D. J. Harrison, W. MacNee, *Am. J. Physiol.*, 1995, **269,** L285-L292.

34 D. R. Riva, C. B. Magalhães, A. A. Lopes, T. Lanças, T. Mauad, O. Malm, S. S. Valença, P. H. Saldiva, D. S. Faffe, W. A. Zin, *Inhal. Toxicol.*, 2011, **23,** 257-267.

35 K. M. P. Pires, M. Lanzetti, C. R. Rueff-Barroso, P. Castro, A. Abrahão, V. L. Koatz, S. S. Valença, L. C. Porto, *Toxicol. in Vitro*, 2012, **26,** 791-798.

36 J. K. W. Chan, S. D. Kodani, J. G. Charrier, D. Morin, P. C. Edwards, D. S. Anderson, C. Anastasio, L. S. Van Winkle, *Am. J. Respir. Cell Mol. Biol.*, 2013, **48,** 114-124.

37 X. Xu, C. Liu, Z. Xu, K. Tzan, M. Zhong, A. Wang, M. Lippmann, L. C. Chen, S. Rajagopalan, Q. Sun, *Toxicol. Sci.*, 2011, **124,** 88-98.

38 L. Hou, X. Zhang, L. Dioni, F. Barretta, C. Dou, Y. Zheng, M. Hoxha, P. A. Bertazzi, J. Schwartz, S. Wu, S. Wang, A. A. Baccarelli, *Part. Fibre Toxicol.*, 2013, **10,** 17.

Figure legends:

Fig. 1 Representative base peak intensity (BPI) chromatograms from A549 cells separated by UPLC/MS under positive (A) and negative (B) ion mode.

Fig. 2 Scoring plots of intracellular metabolites from A549 cells with PCA (A) and PLS-DA (B) model under negative ion mode. ▲ Control; ▲ 30 mg/L; ▲ 60 mg/L.

Fig. 3 Summary of metabolic pathways analyzed with MetaboAnalyst software. 1, nitrogen metabolism; 2, citrate cycle; 3, aminoacyl-tRNA biosynthesis; 4, phenylalanine, tyrosine and tryptophan biosynthesis; 5, glutathione metabolism; 6, glyoxylate and dicarboxylate metabolism.

Fig. 4 Effects of PM2.5 exposure on mRNA expressions of ACO2 (A), IDH2 (B), FH (C) and ATP5C1 (D) genes involved in citrate cycle, and GLUD1 (E) gene involved in glutamate biosynthesis. The data of treatments were calibrated to the control values (control = 1). Values are expressed as means ± SD (n = 6), $^{*}p<0.05$, $^{**}p<0.01$.

Fig. 5 Effects of PM2.5 exposure on mRNA expressions of GPX1 and SOD2 genes involved in oxidative stress. The data of treatments were calibrated to the control values (control = 1). Values are expressed as means ± SD (n = 6), $^{*}p<0.05$, $^{**}p<0.01$.

Fig. 6 Schematic overview of the disturbed metabolic pathways in mitochondria of A549 cells upon PM2.5 exposure. Molecules marked in red represent the differential metabolites detected by metabolomics in the present study.

484 **Table 1** Primer sequences used for real-time PCR analysis

GenBank accession no.	Gene name	Primer sequence (5'→3')
BC026196.2	ACO2	F: CAGGAAATTGAGCGAGGCAA R: CCAACCTGGGCTTCAATCAG
BC071828.1	IDH2	F: AACCGTGACCAGACTGATGA R: GGACTAGGCGTGGGATGTTT
BC017444.1	FH	F: GCAAGCCAAAATTCCTTCCG R: GCTCGCTTCAAGATGCCAAA
BC020824.1	ATP5C1	F: ATCAAGGGGCCTGAAGACAA R: GCAACCTCGCTTTTCATCTG
BC112946.1	GLUD1	F: AAGATCACAAGGAGGTTCACC R: GGTATCAGCGATCCAGGACA
BC070258.1	GPX1	F: TTCGAGAAGTGCGAGGTGAA R: TCAGGCTCGATGTCAATGGT
BC016934.1	SOD2	F: CTGGAACCTCACATCAACGC R: GACCACCACCATTGAACTTCA
BC083511.1	GAPDH	F: GGAGAAGGCTGGGGCTCAT R: TGATGGCATGGACTGTGGTC

Table 2 Identification of differential metabolites detected using UPLC/MS under negative ion mode

HMDB ID	Metabolite	Chemical Formula	Adduct	Measured MW (Da)	Theoretical MW (Da)	MW error (mDa)	VIP value	Change	30 mg/L *vs.* Control		60 mg/L *vs.* Control	
									Average ratio[a]	*P* value[b]	Average ratio[a]	*P* value[b]
HMDB00156	L-Malic acid*	$C_4H_6O_5$	M-H	133.0123	133.0142	1.9	1.75	↓	0.69±0.14	0.006	0.58±0.07	0.001
HMDB00148	L-Glutamic acid*	$C_5H_9NO_4$	M-H	146.0441	146.0459	1.5	1.69	↓	0.63±0.10	0.001	0.66±0.07	0.000
HMDB00159	L-Phenylalanine*	$C_9H_{11}NO_2$	M-H	164.0699	164.0717	1.8	1.69	↑	1.30±0.13	0.020	1.66±0.22	0.000
HMDB00072	cis-Aconitic acid*	$C_6H_6O_6$	M-H	172.9898	173.0092	19.4	1.28	↓	0.67±0.10	0.000	0.42±0.05	0.000
HMDB01138	N-Acetylglutamic acid*	$C_7H_{11}NO_5$	M-H	188.0549	188.0564	1.5	1.33	↓	0.79±0.15	0.009	0.44±0.21	0.000
HMDB00929	L-Tryptophan*	$C_{11}H_{12}N_2O_2$	M-H	203.0811	203.0826	1.5	1.34	↑	1.72±0.23	0.002	2.35±0.31	0.000
HMDB00210	Pantothenic acid#	$C_9H_{17}NO_5$	M-H	218.102	218.1034	1.4	1.81	↓	0.84±0.03	0.002	0.80±0.10	0.000
HMDB00195	Inosine*	$C_{10}H_{12}N_4O_5$	M-H	267.0728	267.0735	0.7	2.76	↓	0.72±0.15	0.008	0.78±0.14	0.028
HMDB11737	Gamma Glutamylglutamic acid#	$C_{10}H_{16}N_2O_7$	M-H	275.0877	275.0885	0.8	1.09	↓	0.54±0.11	0.000	0.49±0.03	0.000
HMDB01067	N-Acetylaspartylglutamic acid#	$C_{11}H_{16}N_2O_8$	M-H	303.0824	303.0834	1.0	1.04	↓	0.79±0.09	0.001	0.71±0.09	0.000
HMDB13220	Beta-Citryl-L-glutamic acid#	$C_{11}H_{15}NO_{10}$	M-H	320.061	320.0623	1.3	3.88	↓	0.69±0.13	0.010	0.62±0.15	0.002
HMDB01227	5-Thymidylic acid*	$C_{10}H_{15}N_2O_8P$	M-H	321.0637	321.0493	14.4	1.16	↓	0.74±0.07	0.000	0.66±0.06	0.000
HMDB60506	S-(2,2-Dichloro-1-hydroxy)ethyl	$C_{12}H_{19}Cl_2N_3O_7S$	M-H	418.0282	418.0248	3.4	1.71	↓	0.64±0.06	0.000	0.58±0.02	0.000

	glutathione[#]											
HMDB01341	ADP[*]	$C_{10}H_{15}N_5O_{10}P_2$	M-H	426.0209	426.0221	1.2	1.72	↓	0.44±0.08	0.000	0.55±0.12	0.002
HMDB06944	1,4-beta-D-Glucan[#]	$C_{18}H_{32}O_{18}$	M-H	535.1529	535.1516	1.3	1.22	↓	0.56±0.23	0.006	0.66±0.21	0.027
HMDB03337	Oxidized glutathione[#]	$C_{20}H_{32}N_6O_{12}S_2$	M-H	611.1431	611.1447	1.6	1.85	↑	3.79±1.15	0.003	4.29±1.66	0.001

[*] Metabolites identified by accurate mass data and MS/MS fragmentation.

[#] Metabolites identified by accurate mass data.

[a] The change of metabolite abundance is expressed as the average ratio of treatment/control (mean ± SD, n = 6). A value >1 represents upregulation whereas a value <1 indicates downregulation.

[b] The statistical significance of abundance change was assessed using ANOVA followed by LSD *post-hoc* test, and $p < 0.05$ was considered as significant.

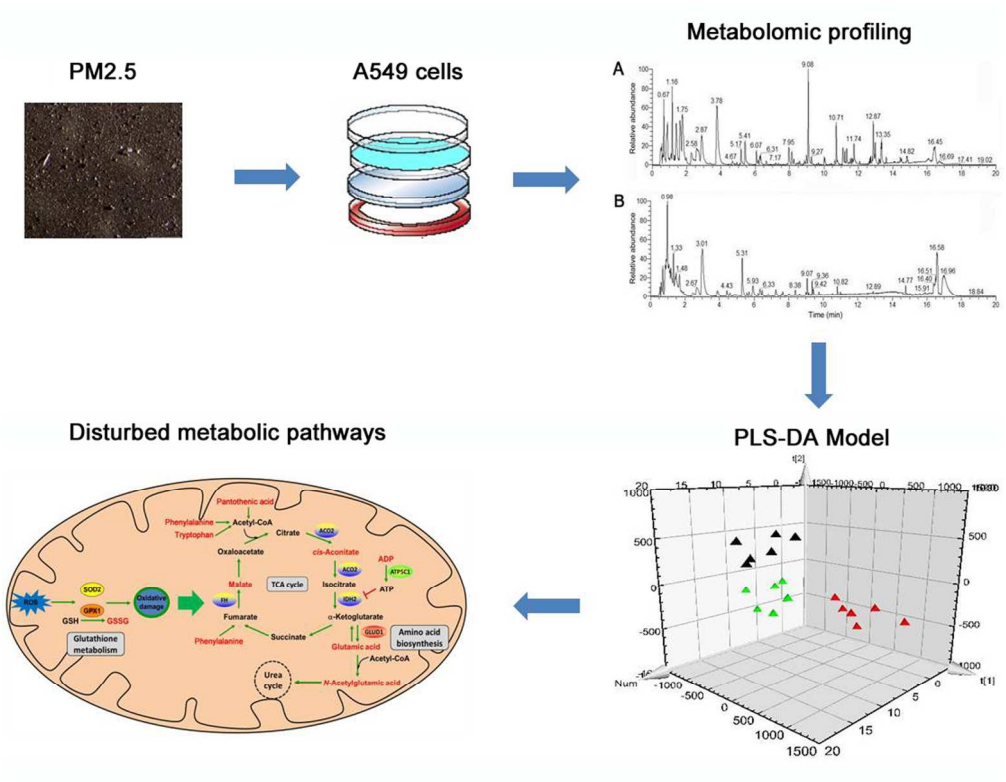

Graphical Abstract: Metabolomics was applied to unravel the metabolome alteration in A549 cells, and citrate cycle, amino acid biosynthesis and glutathione metabolism were the major metabolic pathways disturbed by airborne PM2.5.
188x146mm (300 x 300 DPI)

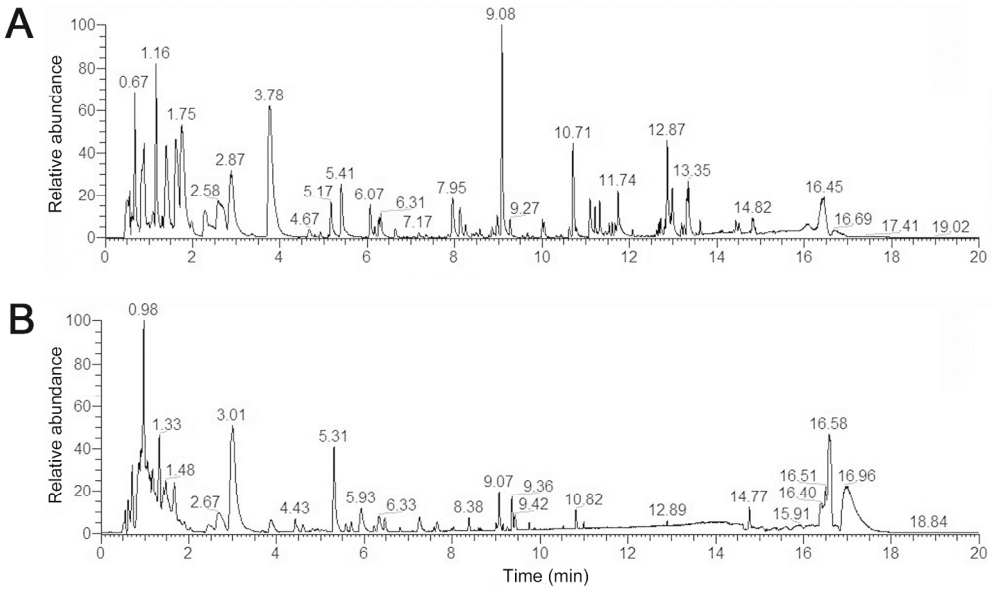

Fig. 1 Representative base peak intensity (BPI) chromatograms from A549 cells separated by UPLC/MS under positive (A) and negative (B) ion mode.
154x92mm (300 x 300 DPI)

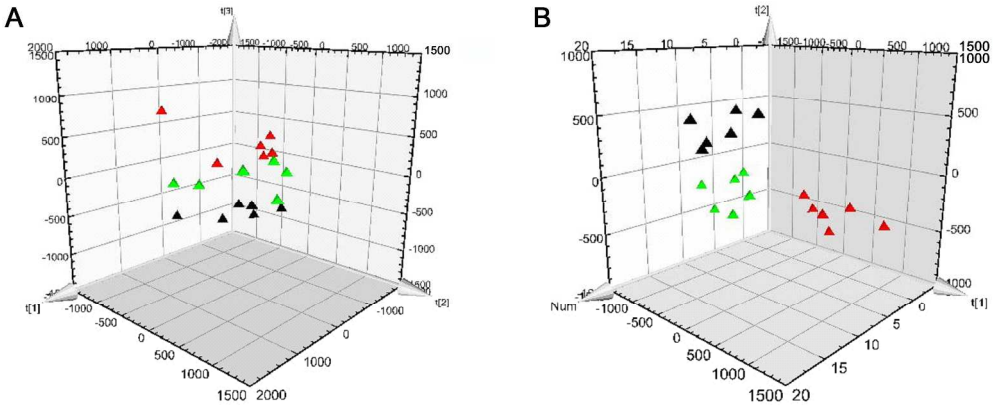

Fig. 2 Scoring plots of intracellular metabolites from A549 cells with PCA (A) and PLS-DA (B) model under negative ion mode. ▲ Control; ▲ 30 mg/L; ▲ 60 mg/L.
315x129mm (300 x 300 DPI)

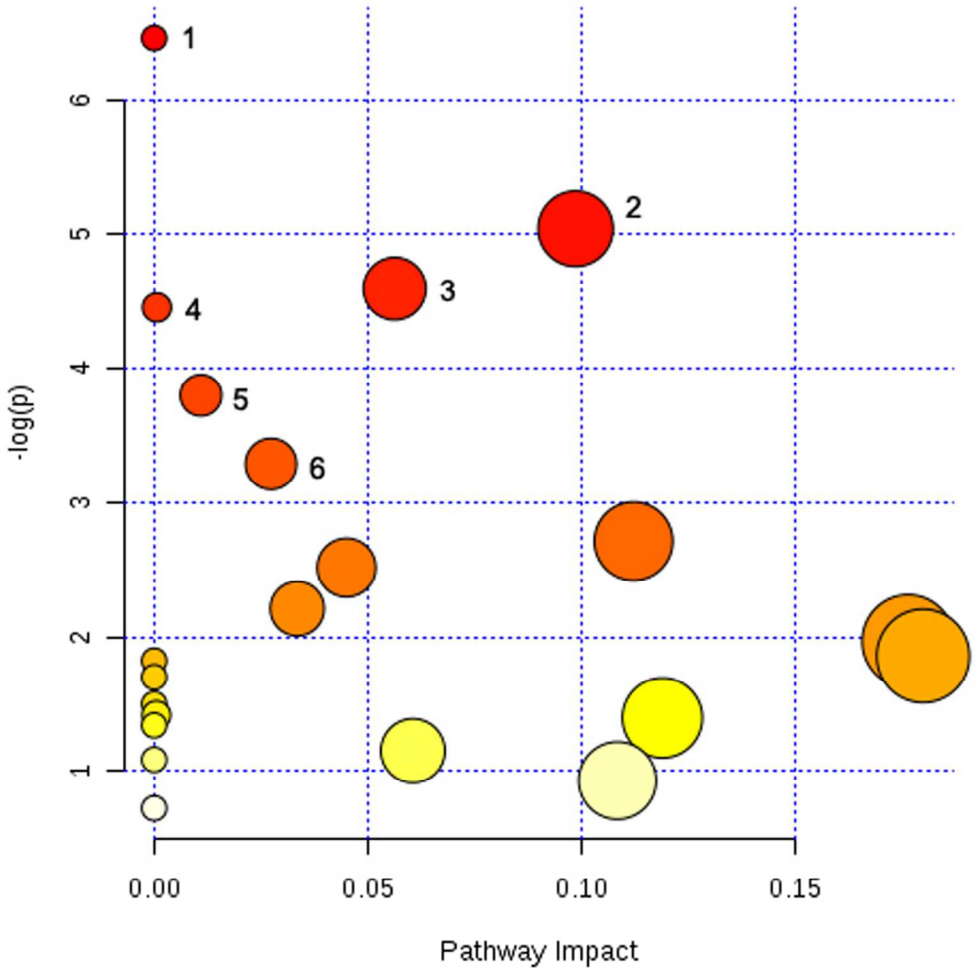

Fig. 3 Summary of metabolic pathways analyzed with MetaboAnalyst software. 1, nitrogen metabolism; 2, citrate cycle; 3, aminoacyl-tRNA biosynthesis; 4, phenylalanine, tyrosine and tryptophan biosynthesis; 5, glutathione metabolism; 6, glyoxylate and dicarboxylate metabolism.
165x163mm (300 x 300 DPI)

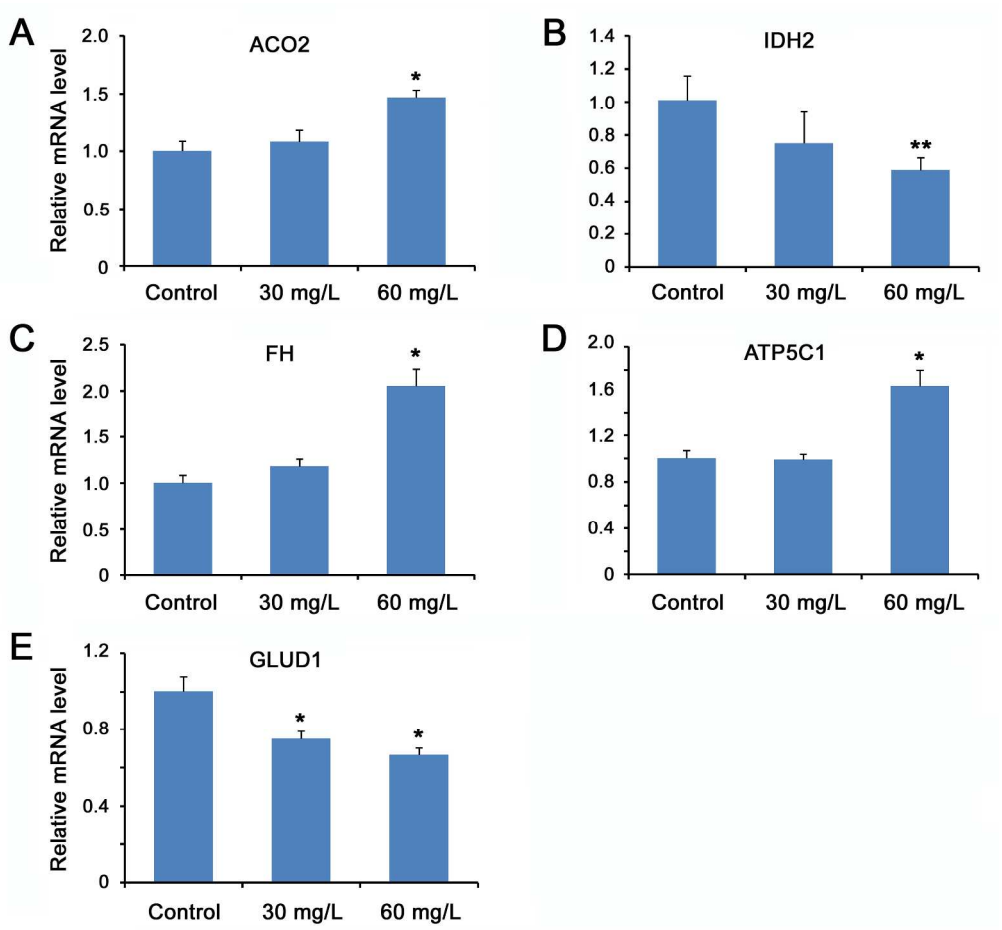

Fig. 4 Effects of PM2.5 exposure on mRNA expressions of ACO2 (A), IDH2 (B), FH (C) and ATP5C1 (D) genes involved in citrate cycle, and GLUD1 (E) gene involved in glutamate biosynthesis. The data of treatments were calibrated to the control values (control = 1). Values are expressed as means ± SD (n = 6), *p<0.05, **p<0.01.
232x215mm (300 x 300 DPI)

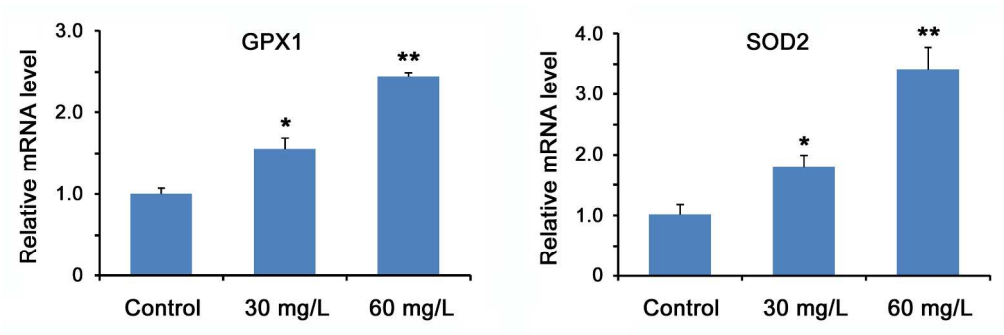

Fig. 5 Effects of PM2.5 exposure on mRNA expressions of GPX1 and SOD2 genes involved in oxidative stress. The data of treatments were calibrated to the control values (control = 1). Values are expressed as means ± SD (n = 6), *p<0.05, **p<0.01.
220x72mm (300 x 300 DPI)

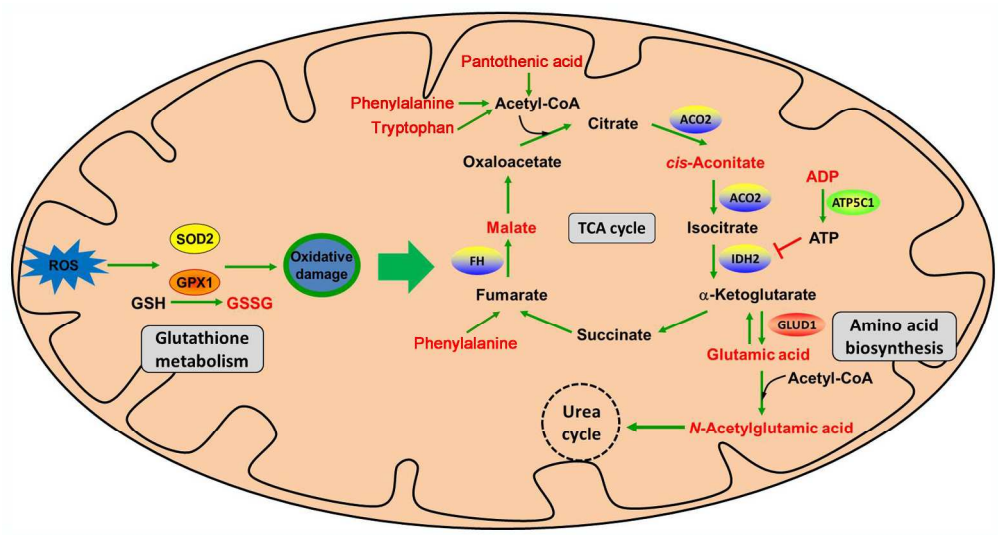

Fig. 6 Schematic overview of the disturbed metabolic pathways in mitochondria of A549 cells upon PM2.5 exposure. Molecules marked in red represent the differential metabolites detected by metabolomics in the present study.
294x157mm (300 x 300 DPI)